Loss of Spatial Control of the Mitotic Spindle Apparatus in a *Chlamydomonas reinhardtii* Mutant Strain Lacking Basal Bodies

Linda L. Ehler, Jeffrey A. Holmes[1] and Susan K. Dutcher

Department of Molecular, Cellular, and Developmental Biology, University of Colorado, Boulder, Colorado 80309-0347

ABSTRACT

The *bld2-1* mutation in the green alga *Chlamydomonas reinhardtii* is the only known mutation that results in the loss of centrioles/basal bodies and the loss of coordination between spindle position and cleavage furrow position during cell division. Based on several different assays, *bld2-1* cells lack basal bodies in >99% of cells. The stereotypical cytoskeletal morphology and precise positioning of the cleavage furrow observed in wild-type cells is disrupted in *bld2-1* cells. The positions of the mitotic spindle and of the cleavage furrow are not correlated with respect to each other or with a specific cellular landmark during cell division in *bld2-1* cells. Actin has a variable distribution during mitosis in *bld2-1* cells, but this aberrant distribution is not correlated with the spindle positioning defect. In both wild-type and *bld2-1* cells, the position of the cleavage furrow is coincident with a specialized set of microtubules found in green algae known as the rootlet microtubules. We propose that the rootlet microtubules perform the functions of astral microtubules and that functional centrioles are necessary for the organization of the cytoskeletal superstructure critical for correct spindle and cleavage furrow placement in Chlamydomonas.

THE position of the mitotic spindle apparatus must be coordinated both temporally and spatially with the cleavage furrow to ensure correct partitioning of the cellular contents. Incorrect placement of these structures with respect to each other would result in cellular catastrophe. The elaborate mechanisms that exist for a cell to monitor the correct replication and segregation of its DNA must act in concert with cleavage furrow positioning. Furthermore, correct segregation of developmental determinants and implementation of developmental programs may require precise cleavage furrow position within cells undergoing development. For example, in *Caenorhabditis elegans*, the specific orientation of the cleavage furrow is necessary for the correct localization of P granules to only one daughter cell in the subsequent division of the P1 cell (HYMAN and WHITE 1987).

The mitotic spindles of many cells are nucleated by the centrosomes, which contain a pair of centrioles/basal bodies and amorphous pericentriolar material (PCM) that usually nucleates a microtubule array (GOULD and BORISY 1977). Although centrosomes appear to be essential for formation of the spindle and the mitotic asters, it is unclear whether the centrioles are necessary for this function. Mouse meiotic spindles do not have centrioles (CALARCO-GILLAM *et al.* 1983),

Corresponding author: Susan K. Dutcher, Department of Molecular, Cellular, and Developmental Biology, University of Colorado, Boulder, CO 80309-0347. E-mail: dutcher@beagle.colorado.edu

[1] *Present address:* Intercampus Program, Molecular Parasitology, 3333 California Street University of California, San Francisco, California, 94143-1204.

Physarum and Naegleria cells do not have centrioles during mycelial growth (FULTON and DINGLE 1971), and higher plant cells do not have centrioles. In addition, the Drosophila haploid tissue culture cell line 1182-4, which was isolated from dead embryos of the female sterile strain mh1182, lacks centrioles when examined by serial thin-section electron microscopy. The cell line undergoes growth and mitotic divisions, but it spontaneously diploidizes, has a high level of aneuploidy and contains large numbers of multinucleate cells (DEBEC *et al.* 1982; DEBEC 1984; SZÖLLÖSI *et al.* 1986). It is unclear whether these defects arise from the lack of centrioles or from the haploid/aneuploid nature of the cell line. In contrast, when the centrioles and most of the pericentriolar material are surgically removed from cells of the monkey cell line BSC-1, an organized array of microtubules is regenerated but centrioles are not, and the cells do not complete cell division (MANIOTIS and SCHLIWA 1991). It is unclear whether the inability of these surgically altered cells to divide is due to a lack of centrioles or to a missing component(s) of the PCM. The evidence for the role of centrioles in cell division remains inconclusive.

The exact mechanisms involved in positioning the mitotic apparatus are unknown. One current model is that the centrosomes migrate to a position previously established or maintained by a microfilament network. The interaction with the actin cytoskeleton is proposed to occur via the astral microtubules that radiate from the centrosomes (HYMAN and WHITE 1987; PALMER *et al.* 1992). In the P blastomeres of *C. elegans*, the centrosomes separate and migrate to positions directly

opposite each other and subsequently both rotate 90 deg to align on the anterior-posterior axis. Rotation of the centrosomes shows sensitivity to microtubule inhibitors (HYMAN and WHITE 1987). Laser irradiation between the centrosome and the cell cortex results in the cessation of centrosomal rotation and implicates a particular cortical site in the rotational events (HYMAN 1989). Treatment of P blastomeres with cytochalasin D, an inhibitor of microfilament assembly, results in the failure of centrosomes to rotate (HILL and STROME 1988, 1990; HYMAN 1989). Actin and actin capping protein have been shown to transiently accumulate at a cortical site that also has astral microtubules in its vicinity during the time of centrosomal rotation; blastomeres that do not undergo centrosomal rotation do not accumulate capping protein at this site (WADDLE et al. 1994).

In the budding yeast, Saccharomyces cerevisiae, characterization of strains that have abnormal placement of the mitotic apparatus has implicated astral microtubules, cytoplasmic dynein, dynactin complex, and actin microfilaments in establishing or maintaining the spindle in the correct position before anaphase. At the restrictive temperature, the β-tubulin mutant strain tub2-401 loses astral microtubules preferentially, the mitotic spindles misorient; anucleate and multinucleate cells accumulate (HUFFAKER et al. 1988; SULLIVAN and HUFFAKER 1992). Deletion mutations in the cytoplasmic dynein heavy chain gene DHC1 (DYN1) or JNM1 result in minor spindle orientation defects (ESHEL et al. 1993; LI et al. 1993; McMILLAN and TATCHELL 1994). Spindle misorientation in dhc1 (dyn1) disruption strains is accompanied by elongated astral microtubules and an increase in cells that are binucleate. Act5 is a member of the actin-related protein family Arp1 and is homologous to the actin-like protein found in the vertebrate dynactin complex. Deletions of the ACT5 gene result in minor spindle placement defects (GILL et al. 1991; MUHUA et al. 1994).

Several lines of evidence suggest that the position of the cleavage furrow is determined by the position of the mitotic apparatus. The furrow always forms at right angles to the spindle, bisecting it and can be repositioned by moving the mitotic apparatus before the end of anaphase (reviewed in RAPPAPORT 1986). In par mutant strains of C. elegans, the mitotic apparatus fails to migrate to its normal position and the subsequent furrow forms in a position corresponding to the abnormal location of the spindle (KEMPHUES et al. 1986, 1988; CHENG et al. 1995). A furrow always forms between the two asters of the spindle, regardless of the original position of the mitotic apparatus. Experiments performed on invertebrate oocytes have shown that a cleavage furrow can form between asters that belong to different mitotic spindles, as long as the asters are within a maximum distance of each other (RAPPAPORT 1961) and all regions of an aster are equally effective in generating a furrow (reviewed in RAPPAPORT 1986). Cleavage furrow

formation is dependent on microtubules; loss of microtubules from treatment with colchicine before midanaphase prevents cleavage furrow initiation (BEAMS and EVANS 1940; HAMAGUCHI 1975). These results suggest that the asters and probably the astral microtubules play a key role in positioning the cleavage furrow.

We have characterized a C. reinhardtii mutant strain, bld2-1, that lacks centrioles/basal bodies. The strain was originally isolated by GOODENOUGH and ST. CLAIR (1975), has a single genetic lesion, and represents the first allele at a previously unidentified locus. Cells lack centrioles/basal bodies in >99% of the population and GOODENOUGH and ST. CLAIR (1975) proposed that the BLD2 gene product is required for the formation of doublet and triplet microtubules. In addition to the basal body defect, we have found that cellular organization is disrupted. The placement of the mitotic spindle is no longer correlated spatially or temporally with the cleavage furrow and is misplaced relative to the stereotyped cytological position seen in wild-type cells. The position of the cleavage furrow is also aberrant, but it always colocalizes with specialized structures known as rootlet microtubules. The rootlet microtubules in bld2-1 cells are disorganized and often mispositioned in relation to the mitotic spindle. These observations clearly implicate the BLD2 gene product as a component involved in the correct positioning of the mitotic spindle. The role of the BLD2 gene product may be in the initiation or structure of functional centrioles, which may be necessary to maintain the elaborate cytoskeletal organization critical for correct cell division in C. reinhardtii.

MATERIALS AND METHODS

Strains and culture conditions: The 137c mt$^+$ strain of C. reinhardtii was used as the wild-type strain for this study unless otherwise noted. The bld1-1 and the bld2-1 strains were originally isolated by GOODENOUGH and ST. CLAIR (1975) and obtained from the Chlamydomonas Genetics Center. The aflagellate strain 426 was isolated in a screen for cells that could not swim after heat shock treatment (42°, 30 min) of a member of the F$_1$ generation from a cross of strain 137c to the polymorphic strain, CC1952 (GROSS et al. 1988). Cultures were usually grown under constant illumination on agar plates or in liquid medium at 21° as described previously (LUX and DUTCHER 1991). To obtain a higher percentage of cells in division, two methods were used. First, wild-type cells at very low density were inoculated into a 2-liter separatory funnel with 1.5 liter of minimal medium (medium I of SAGER and GRANICK 1954) and grown at 21° under constant illumination of 25 μE/m^2/sec until the culture was slightly green. The funnel was then wrapped in foil except for 1 inch at the top and cells were allowed to accumulate in the light for 2 hr. Culture medium (100 ml) was then removed from the bottom of the funnel. Twenty percent of cells in this fraction were dividing. In the second method, bld2-1 and wild-type cells were inoculated at low density into flasks containing minimal medium at 21° with constant stirring until achieving log phase growth. Cells were then resuspended in fresh minimal medium and fixed after 14 hr when ~10% of cells were dividing. Deflagellation of wild-type cells was performed as described in WITMAN et al. (1972).

Mating of Chlamydomonas strains: Mating of flagellated cells was performed as described by HARRIS (1989). Aflagellate cells were induced to mate with the addition of dibutryl cyclic adenine monophosphate (cAMP) and the phosphodiesterase inhibitor 3-isobutyl-1-methylxanthine to the medium (PASQUALE and GOODENOUGH 1987; DUTCHER 1995).

Mapping of the bld2-1 allele: The bld2-1 allele is unlinked to all linkage groups except linkage group III (data not shown). The BLD2 locus maps to linkage group III in crosses to NIT2, AC17, and TUA1: bld2-1-ac17-1: 33:0:7; bld2-1-nit2: 66:0:3; bld2-1-tua1-1: 46:0:11. Three point crosses between bld2-1, nit2, and tua1-1 indicate that BLD2 is distal to both NIT2 and TUA1.

Reversion of the bld2-1 allele: Ultraviolet irradiation (UV) and ethyl methyl sulfonate (EMS) mutageneses were performed as described in LUX and DUTCHER (1991), except that cells were grown at 21° and four transfers were performed. In a separate mutagenesis, log phase cultures were exposed to a ^{137}Cs gamma (γ) irradiation source (J. L. S. Shepherd and Associates, model 143) at 498R/min for 30 min. After irradiation, cultures were treated as for the UV and EMS mutageneses.

Microscopic techniques: Observations were made and images photographed on a Zeiss Axiophot microscope equipped with a ×100 plan-Neofluor objective. Several different antibodies were used in this study. The monoclonal antibody 3A5 is specific for all forms of α-tubulin tested, was used at a 1:10 dilution, and was a gift from M. T. FULLER (Stanford University) and J. R. MCINTOSH (University of Colorado, Boulder). The monoclonal antibody 6-11B-1 is specific for acetylated α-tubulin (LEDIZET and PIPERNO 1986), was used at a 1:50 dilution, and was purchased from Sigma Chemical Co. The monoclonal antibody 17E10 is specific for centrin, was used at a dilution of 1:500, and was a gift from J. L. SALISBURY (Mayo Clinic). The polyclonal anti-Volvox actin antibodies were generated against the conserved amino-terminal decapeptide of Volvocalean algal actin and have been shown by Western blot analysis to specifically recognize the 43-kD C. reinhardtii actin protein with no cross reactivity (GARDNER et al. 1994). This antibody was used at a 1:20 dilution and was a gift from D. KIRK (Washington University). Centrin staining was performed as described in SALISBURY et al. (1988). Staining for tubulin alone was as described by HOLMES and DUTCHER (1989). Double labeling with actin and tubulin antibodies was performed using the protocol described by HARPER et al. (1992). Secondary antibodies were Texas Red-goat anti-mouse IgG (Molecular Probes), and FITC-goat anti-rabbit IgG (Zymed). Standard control experiments were performed and no aberrant labeling or cross reactivity of any secondary antibodies was observed (data not shown). DAPI was used in water at 0.2 μg/μl final concentration.

Identification of mitotic stages: Assessment of mitotic stages was based on the shape, position, and appearance of the DAPI-stained DNA, as well as the conformation of the mitotic spindle. Designation of prometaphase normally involves distinct assessment of the attachment of kinetochores to spindle microtubules; this was not possible in these experiments. Therefore, the assessment of prometaphase was determined by slight differences in DNA shape and spindle morphology from metaphase and is somewhat subjective. In mammalian cells, telophase is usually defined by the reformation of the nuclear envelope. Because the nuclear envelope does not completely break down in C. reinhardtii, no attempt was made to identify this stage. The telophase stage identified by previous authors by the absence of the mitotic spindle or the close position of the nuclei to each other (GAFFEL and EL-GAMMEL 1990; HARPER et al. 1992) was scored as cytokinesis in this study, as cleavage furrows are present in such cells.

Meiotic progeny experiment: After mating, zygotes were placed on solid agar medium for 18 hr in the light and then placed in the dark for ≥3 days. Plates were then exposed to chloroform vapors for 45 sec; nonzygotic cells are killed by this treatment. Zygotes were placed in liquid medium and allowed to germinate. The presence of flagella was monitored over time by microscopic examination of the cells.

RESULTS

Cellular organization and division in Chlamydomonas: The highly stereotyped organization of the Chlamydomonas cytoskeleton results in a precise, structured organization of cell division. The interphase microtubule organizing center (MTOC) is located at the anterior of the cell and consists of the basal bodies, four specialized microtubules known as rootlet microtubules, and the nucleus-basal body connector (Figure 1). Each basal body nucleates a flagellum and is associated with two rootlet microtubules, one of which contains two tubules and the other four tubules (RINGO 1967; JOHNSON and PORTER 1968; GOODENOUGH and WEISS 1978; MOESTRUP 1978). The four rootlet microtubules are positioned in a cruciate pattern; they extend toward the posterior of the cell just underneath the plasma membrane. The remaining cytoplasmic microtubules extend from the vicinity of the basal bodies and rootlets and form a cup-shaped pattern with the basal bodies as the base. During mitosis, the duplicated pairs of centrosomes and their old rootlet microtubules migrate away from each other to the future poles of the mitotic spindle and the basal bodies become centrioles; the cytoplasmic microtubules and flagella disassemble (LEDIZET and PIPERNO 1986). The direction of migration of the basal bodies and rootlet microtubules results in the positioning of the mitotic spindle perpendicular to the anterior-posterior axis in the anterior of the cell (Figure 2) (GAFFEL and EL-GAMMEL 1990). During the migration of the basal bodies, the four-membered rootlet microtubules bend at approximate right angles. The distal portions of the rootlets orient perpendicularly to the spindle and the proximal portions are parallel to the spindle (Figure 2, prophase). In anaphase, new microtubule arrays begin to form perpendicularly between the nuclei; they originate from the four-membered rootlet microtubules (JOHNSON and PORTER 1968; GAFFEL and EL-GAMMEL 1990; SCHIBLER and HUANG 1991).

These microtubules spread to the interior of the cell by telophase and together with the four-membered rootlet microtubules form the phycoplast. The cleavage furrow forms along the phycoplast in a position that is correlated cytologically with the position of the distal ends of the parental four-membered rootlet microtubules and proceeds from the anterior of the cell to the posterior (HOLMES and DUTCHER 1989). The precise positioning of the rootlet microtubules in relation to the spindle is therefore correlated with the exact positioning of the cleavage furrow that divides the cell into equal halves.

trans flagellum   cis flagellum

basal bodies

nucleus–basal body
connector

nucleus

4–membered
rootlet
microtubules

2–membered
rootlet
microtubules
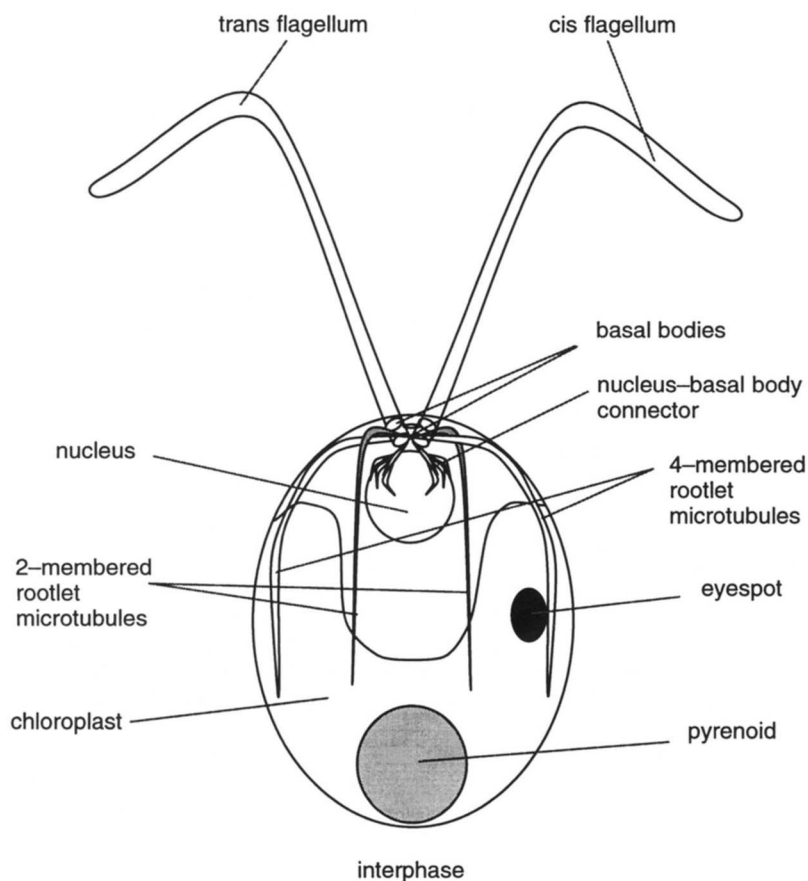
eyespot

chloroplast

pyrenoid

interphase

FIGURE 1.—Diagram of interphase cell morphology of *C. reinhardtii*. The microtubule organizing center consists of two flagella, two mature basal bodies with associated probasal bodies (not shown), and two sets of rootlet microtubules. The nucleus-basal body connector extends from the basal bodies to the nucleus. The eyespot is always associated with the *cis* four-membered microtubule rootlet. The pyrenoid serves as a cellular landmark for the stereotypical organization of the cells in these experiments. The cytoplasmic microtubules and the pericentriolar material are not included in this diagram.

Genetic characterization of the *bld2* strain: The *bld2-1* strain (previously designated *bald-2*) is aflagellate and was isolated in a screen for cells unable to mate because flagella are required for mating in Chlamydomonas (GOODENOUGH and ST. CLAIR 1975). However, this requirement can be bypassed by artificially raising the intracellular cAMP levels (PASQUALE and GOODENOUGH 1987). Between 0.5–30% of the *bld2-1* cells mated with wild-type cells under these conditions to form zygotes. The aflagellate phenotype of *bld2-1* cells showed Mendelian segregation in 550 tetrads and is therefore likely to result from a single gene mutation. Greater than 96% of the meiotic progeny from these crosses were viable, which suggests that the mutation does not have a dominant effect on meiotic viability and that there are no unlinked modifiers of a growth or cell cycle phenotype in *bld2-1* strains. The *BLD2* locus mapped 9.5 cM to the left of the centromere of linkage group III (see MATERIALS AND METHODS). The *bld2-1* mutation also conferred a recessive meiotic phenotype; homozygous *bld2-1* zygotes failed to germinate at all temperatures tested from 16 to 32°. This phenotype cosegregated with the aflagellate phenotype in 75 tetrads. The *bld2-1* mutation was recessive to the wild-type allele in stable heterozygous diploid strains for the phenotypes described below (data not shown). Dominance of actin localization and temporal control was not determined.

Penetrance of the aflagellate phenotype in *bld2-1*

strains: Several methods were used to confirm that *bld2-1* cells lack flagella and basal bodies. By light microscopic examination, *bld2-1* cells were completely aflagellate ($n = 5000$). As mentioned above, mating between Chlamydomonas cells normally requires the presence of flagella, and we failed to detect any mating between 10^8 wild-type and 10^8 *bld2-1* cells, which suggested that none of the *bld2-1* cells have flagella. GOODENOUGH and ST. CLAIR (1975) examined the *bld2-1* strain by electron microscopy and found that most cells lack an assembled basal body. We examined two aflagellate meiotic progeny from our backcrossed strains by serial thin-section electron microscopy and no basal bodies were detected in these cells or in ~1000 random thin sections (data not shown).

The examination of *bld2-1* cells by immunofluorescence allowed us to examine a larger number of cells for the presence of basal bodies. Using indirect immunofluorescence with an antibody against acetylated α-tubulin that stains basal bodies and rootlet microtubules (LEDIZET and PIPERNO 1986), we examined deflagellated wild-type cells, a control aflagellate strain (426), and *bld2-1* cells. Deflagellation removes flagella at the cell wall and leaves the basal bodies intact. In 90% of deflagellated wild-type cells and in strain 426, two dot-like structures at the anterior end of the cell and the rootlet microtubules were stained with the antibody (Figure 3, a and b). In *bld2-1* cells, acetylated mi-

basal bodies

nucleus

4–membered rootlet microtubules

2–membered rootlet microtubules

eyespot

actin

pyrenoid

interphase

telophase/cytokinesis
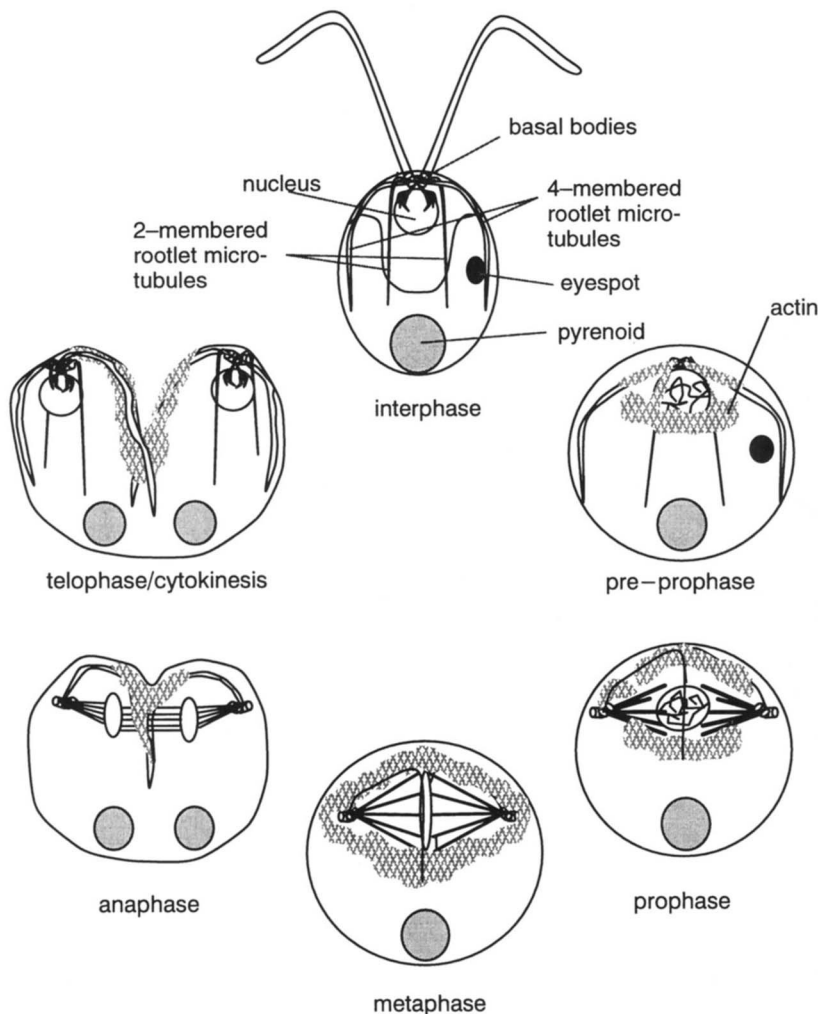
pre–prophase

anaphase

prophase

metaphase

FIGURE 2.—Diagrammatic representation of the distribution of actin in relation to the spindle and rootlet microtubules during wild-type cell division in Chlamydomonas. Interphase: the centrioles are found in a perinuclear location and function as basal bodies for the assembly of flagella. Each basal body is associated with a two- and a four-membered microtubule rootlet throughout the cell cycle. Preprophase: the DNA is condensed and the flagella are disassembled. The rootlets and basal bodies have not yet migrated. Actin colocalizes with the proximal portions of the rootlets and appears in a ring around the nucleus at the anterior of the cell. Prophase: the DNA is condensed but not aligned at the metaphase plate. The spindle has begun to form but appears incomplete. Actin is distributed in a diffuse ring that does not appear to overlap the spindle. The eyespot has begun to breakdown. Metaphase: the DNA aligns along the metaphase plate; the spindle is fully formed. Actin is distributed in a ring around the spindle. Anaphase: the DNA separates; the spindle appears elongated. A small cleavage furrow is sometimes apparent and the actin appears distributed along the rootlets and the incipient furrow. Telophase/cytokinesis: the DNA moves back toward the furrow; the MTOCs appear fully formed with a full complement of rootlets; the parental four-membered rootlets are coincident with the furrow. The phycoplast has formed and actin is concentrated at the furrow.

crotubules were stained, but no staining of two dot-like structures was detected in 2000 cells (Figure 3c).

To confirm these observations, wild-type cells were stained with an antibody against centrin. Centrin is a calcium-binding protein that localizes to the fibrous nucleus-basal body connector and the distal striated fiber between basal bodies (SALISBURY *et al.* 1988). Anticentrin staining of wild-type cells and cells from another aflagellate strain, *bld1-1,* showed a pattern of two ribbons that connect the nucleus to the basal bodies where they are connected by an additional band of staining; this pattern has been referred to as the "diamond ring" (Figure 3d) (WRIGHT *et al.* 1985). Cells without basal bodies are unlikely to have distal striated fibers and an extended nucleus-basal body connector. About 0.5% of the *bld2-1* cells observed have the wild-type diamond ring morphology (*n* = 2000; Figure 3e). It is likely that there is sufficient basal body structure to assemble the centrin fibers in this subset of cells.

GOODENOUGH and ST. CLAIR (1975) observed that a small fraction of *bld2-1* cells had rings of singlet microtubules; these cells may correspond to the cells with extended centrin fibers.

Coreversion analysis of *bld2-1*: To determine if the flagellar and cytoskeletal organizational phenotypes described in the following sections were the consequence of the same mutation, we analyzed the coreversion of these phenotypes. We isolated revertants/suppressors of the aflagellate phenotype using enrichment screens for cells that regained the ability to assemble functional flagella and therefore could swim in liquid cultures. Without mutagenesis, no swimming cells were recovered in 5×10^9 *bld2-1* cells. We obtained 15 revertants following UV irradiation, three revertants from γ irradiation and 22 from treatment with EMS in four independent experiments. Each revertant was crossed to a wild-type strain to determine if the reversion event was intragenic or extragenic. In all 40 revertants, the reversions appeared to result from an intragenic or closely linked event (Table 1). The likely intragenic nature of the reversion events was best illustrated in strains UV1-8R, UV1-11R, and γ1-1R, in which the second event is at most 0.1, 0.37, and 0.4 cM, respectively, from the original *bld2-1* lesion (Table 1). The UV and γ irradiation-induced mutations were indistinguishable from wild-type cells based on swimming patterns, phototactic behaviors, and mitotic doubling times at temperatures from 16 to 32°. Therefore, all phenotypes examined in Table 1 appear
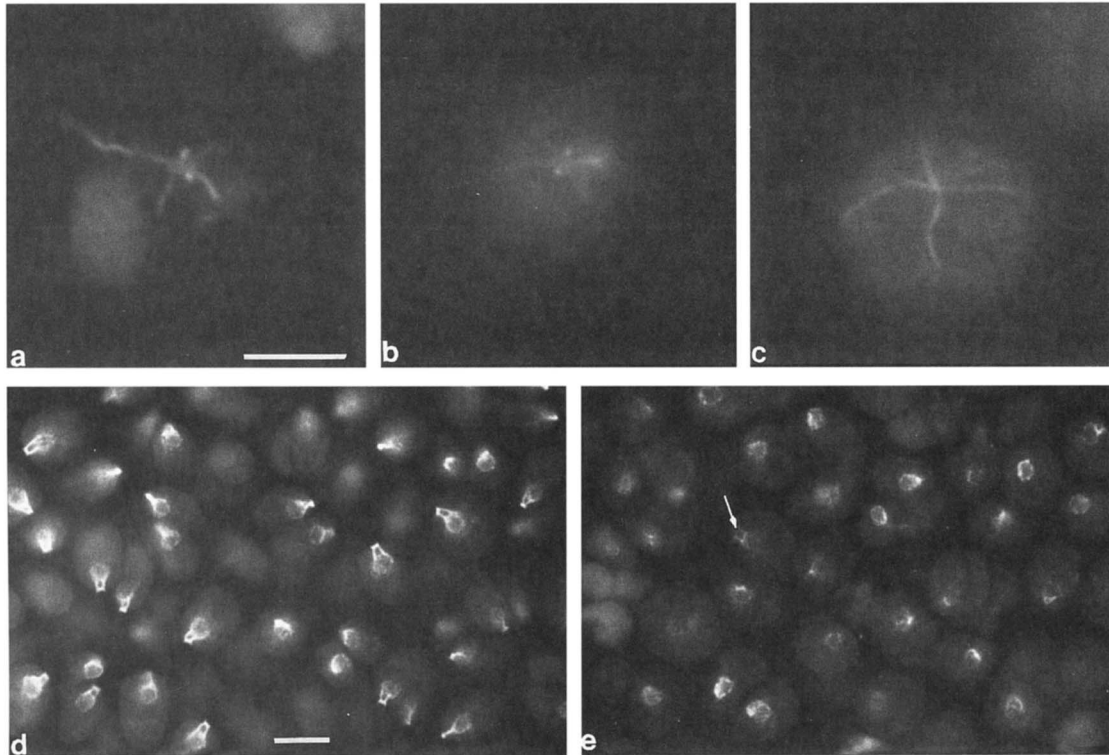
FIGURE 3.—Immunofluorescent staining of interphase cells. (a–c) Cells were stained with anti-acetylated α-tubulin antibody and with FITC-conjugated secondary antibody. (a) Deflagellated wild-type cells. The acetylated microtubules appear in a cruciate pattern and two dot-like structures that are in positions that correlate to the expected position of basal bodies are clearly visible ($n =$ 200). (b) Aflagellate strain 426. The acetylated microtubules appear in the wild-type cruciate pattern with the two dot-like structures clearly visible. (c) *bld2-1*. The acetylated microtubules appear disorganized and abnormal in number and no dot-like structures are observed. (d and e) Cells were stained with anti-centrin antibody and FITC-conjugated secondary antibody. (d) *bld1-1* cells are aflagellate, but have basal bodies, and show the normal "diamond ring" pattern of wild-type centrin distribution. (e) *bld2-1* cells show centrin staining, but very few cells have the "diamond ring" associated with extended centrin fibers (arrow). Bars = 10 μm.

to arise from the *bld2-1* allele. Interestingly, six of the revertants recovered after treatment with EMS acquired an altered swimming phenotype that was tightly linked to the Bld2⁻ aflagellate phenotype (Table 1). This aberrant swimming may arise from flagella that are incorrectly templated or that are defective in structure.

Rescue of the aflagellate phenotype in dikaryons: We examined *bld2-1* × *BLD2* transient dikaryons to determine if the components that are necessary and sufficient to assemble basal bodies were present in gametic cells. If so, then wild-type cytoplasm might be able to rescue the aflagellate phenotype of *bld2-1* cells. During mating in Chlamydomonas, parental cells fuse within 5–10 min and the resulting dikaryons remain in the G_0 interval of the cell cycle for ~1.5-2 hr, during which the haploid nuclei fuse and the program of zygotic gene expression commences (ARMBURST *et al.* 1993). During this interval, most mutant strains that have aberrant motility or defects in the assembly of flagellar structures are rescued by the presence of wild-type cytoplasm (STARLING and RANDALL 1971; LUCK *et al.* 1977; DUTCHER *et al.* 1984).

In populations of *bld2-1* × *BLD2* mating cells in which zygotes were later recovered at a frequency of 10%, no quadriflagellate cells were observed by light microscopy

up to 2 hr after mixing of the parental cells. To increase our ability to detect rescue of the aflagellate phenotype, a phototaxis assay was used that specifically monitored the behavior of dikaryons. Dikaryons were distinguished from unmated haploid cells based on the observation that zygotic cell walls adhere to one another to form a pellicle. Phototactic dikaryons will form a pellicle that adheres to the glass wall of a test tube at the point of light incidence. Zygotes formed from dikaryons that were not phototactic formed a pellicle, but did not concentrate at the point of light incidence. The ability of *bld2-1* dikaryons to undergo phototaxis when mated to wild-type cells or to *pf18* cells was tested. Cells with the *pf18* mutation have a paralyzed flagellar phenotype that is not rescued in dikaryons (STARLING and RANDALL 1971). Homozygous *pf18* dikaryons were not phototactic while heterozygous dikaryons were, which suggests that a single pair of flagella was sufficient for phototaxis (Figure 4). Dikaryons formed in crosses of *bld2-1* with wild-type cells performed phototaxis; the *bld2-1* mutation did not have a negative effect on phototaxis. Dikaryons formed in crosses of *bld2-1* and *pf18* were not phototactic, although dikaryons were formed as confirmed by the presence of the pellicle. This suggested that motile flagella were not assembled and that the *BLD2* cyto-

TABLE 1

Coreversion of *bld2-1* phenotypes in intragenic revertant strains

Isolation name	No. tetrads examined	Coreversion[a]			Swimming phenotype[b]
		Cytokinesis	Eyespot placement	Rootlet MT	
UV1-1R	34	+	+	ND	+
UV1-2R	17	+	+	ND	+
UV1-3R	31	+	+	ND	+
UV1-4R	15	+	+	ND	+
UV1-5R	29	+	+	ND	+
UV1-6R	49	+	+	ND	+
UV1-7R	16	+	+	ND	+
UV1-8R	510	+	+	+	+
UV1-9R	17	+	+	ND	+
UV1-10R	50	+	+	ND	+
UV1-11R	136	+	+	+	+
UV1-12R	17	+	+	ND	+
UV1-13R	52	+	+	ND	+
UV2-1R	60	+	+	ND	+
UV2-2R	31	+	+	ND	+
γ1-1R	125	+	+	+	+
γ2-1R	18	+	+	ND	+
γ2-2R	34	+	+	ND	+
EMS7-1	25	+	+	+	Aberrant[c]
EMS7-2	35	+	+	+	+
EMS7-3	14	+	+	+	+
EMS7-4	17	+	+	+	+
EMS7-5	12	+	+	+	+
EMS7-6	18	+	+	+	+
EMS8-5	32	+	+	+	+
EMS8-6	16	+	+	+	+
EMS8-7	13	+	+	+	+
EMS9-1	15	+	+	+	+
EMS9-2	33	+	+	+	+
EMS9-3	19	+	+	+	+
EMS9-4	31	+	+	+	Aberrant[c]
EMS9-5	32	+	+	+	Aberrant[c]
EMS9-6	32	+	+	+	+
EMS10-3	33	+	+	+	Aberrant[c]
EMS10-4	98	+	+	+	Aberrant[c]
EMS10-5	34	+	+	+	Aberrant[c]
EMS10-7	13	+	+	+	+
EMS10-8	15	+	+	+	+
EMS10-9	17	+	+	+	+
EMS10-11	16	+	+	+	+

ND, not determined.

[a] Revertant strains were crossed by wild-type cells and tetrad progeny were examined for the cosegregation of flagella, cytokinetic fidelity, eyespot placement, rootlet number and placement, and any new phenotype exhibited by the revertant strain. Cytokinesis was observed by phase microscopy ($n = 100$), eyespot position was examined by DIC microscopy ($n = 100$), and rootlets were examined by immunofluorescence ($n = 20$) using the antibody against acetylated α-tubulin. In addition, the number of nuclei per cell ($n = 100$) and daughter cell size ($n = 25$) were also scored and were reverted in all strains examined. + indicates reversion.

[b] Swimming phenotypes were assessed as compared with wild type; + indicates no difference from wild type.

[c] Linkage of abnormal swimming to the *BLD2* locus was tested in crosses to the *bld2-1* strain and in all cases the swimming phenotype was tightly linked ($n = 20$–30 tetrads each).

plasm contributed from the *pf18* parent was unable to rescue the aflagellate phenotype; however, we cannot rule out the unlikely possibility that nonmotile flagella were assembled in a small, microscopically undetected fraction of the dikaryons.

Rescue of the aflagellate phenotype in meiotic prog-

eny: To determine if the components that are necessary and sufficient to assemble basal bodies were present in *bld2-1* cells during or directly after meiosis in the initial mitotic divisions, we examined the phenotype of cells that had just completed meiosis. Heterozygous *BLD2/ bld2-1* zygotes were germinated and the presence

Parental Strains	Dikaryon Phototaxis	Observed Phenotype
wild–type x wild–type	+	four normal flagella
wild–type x *pf18*	+	two normal flagella, two paralyzed flagella
wild–type x *bld2–1*	+	two normal flagella
pf18 x *bld2–1*	−	two paralyzed flagella[a]

FIGURE 4.—Dikaryon phenotypes of *bld2-1* strains. *BLD2* cells were mated to *bld2-1* cells and the resulting dikaryons were assayed for their ability to perform phototaxis. Formation of dikaryons was scored by the subsequent presence of zygotes. The ability of dikaryons to phototax was scored by the presence or absence of zygotes at the point of light incidence (see MATERIALS AND METHODS). [a]Due to low mating efficiency, this phenotype was not observed directly.

of flagella was monitored over time by microscopic examination. Because each zygote will produce two zoospores with the wild-type genotype and two zoospores with the *bld2-1* genotype, 50% of cells examined should have flagella. If there is rescue of the aflagellate phenotype then >50% of cells will have flagella. After the first mitotic division, >70% of the meiotic progeny had flagella ($n = 500$ cells; Figure 5). The homozygous *BLD2* control meiotic progeny had a similar percentage of flagellated cells ($n = 500$). The presence of flagella on meiotic progeny decreased over time, so that after approximately four to five generations, ~45% of cells were flagellated. No increase in the number of uniflagellate cells was observed. Therefore, genotypically *bld2-1* cells assembled basal bodies during meiosis from the cytoplasm contributed from the *BLD2* parent and maintained them for a limited number of generations after
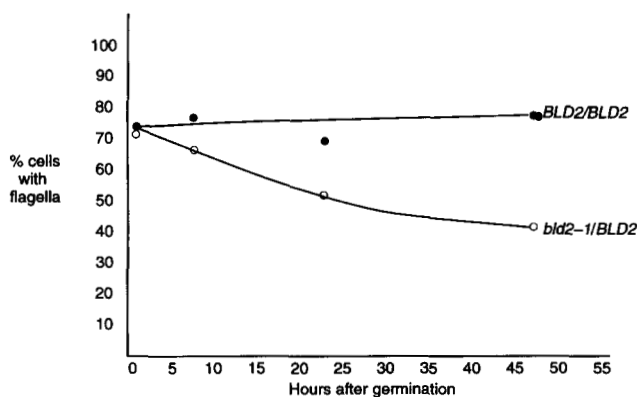

FIGURE 5.—Rescue of the Bld⁻ aflagellate phenotype in meiotic progeny. *BLD2/BLD2* and *BLD2/bld2-1* zygotes were placed in liquid medium and allowed to germinate. Zygotes germinated at ~16 hr after exposure to light. The number of cells with flagella was monitored over time by light microscopy. Each point represents an average of the number of cells with flagella at the median time point for two experiments. The doubling times of individual meiotic progeny were monitored over the course of the experiment and were indistinguishable from each other. Five hundred cells were counted for each time point in each experiment.

germination. The phenotypic rescue in postmeiotic cells suggests the *BLD2* gene does not need to be transcribed in each cell cycle. However, the introduction of wild-type cytoplasm to G_0 arrested cells was not sufficient to provide rescue (see above). One explanation for these observations is that the BLD2 gene product may be a component of a structure that is not normally assembled in G_0, such as the basal body annulus (GOULD 1975).

Eyespot and rootlet microtubule placement in *bld2-1* cells: In each cell cycle, the eyespot is disassembled. After mitosis, each daughter assembles a new eyespot opposite the cleavage furrow in close association with a newly formed rootlet microtubule (HOLMES and DUTCHER 1989). Both wild-type and aflagellate *bld1-1* cells assembled new eyespots opposite the cleavage furrow ($n = 500$). In contrast, *bld2-1* cells contained eyespots that were not on the cell equator or opposite the cleavage furrow in 45% of the dividing pairs ($n = 500$). Because the eyespot is found in an exact cellular location with respect to the four-membered rootlet microtubules in wild-type cells, it was possible that the abnormal positioning of the eyespot in *bld2-1* cells was associated with a defect in the placement of the rootlet microtubules. The rootlet microtubules of *bld2-1* and wild-type cells were stained using the antibody against acetylated α-tubulin. The stereotyped cruciate organization of rootlet microtubules observed in wild-type cells (HOLMES and DUTCHER 1989) was absent in most *bld2-1* cells; both the placement and the number of rootlet microtubules were abnormal (Figure 3c). During mitosis and cytokinesis of *bld2-1* cells, the rootlet microtubules were often mispositioned (see below).

Fidelity of cleavage furrow placement in *bld2-1* cells: The position of the cleavage furrow is always correlated with the four-membered rootlet microtubules in wild-type cells (JOHNSON and PORTER 1968; HOLMES and DUTCHER 1989; GAFFEL and EL-GAMMEL 1990). Therefore, it was possible either that the position of the cleavage furrow was disassociated from the rootlet microtu-

bules in *bld2-1* cells or that the cleavage furrow was mispositioned along with the mispositioned rootlet microtubules. The location of the cleavage furrow in relation to the rootlet microtubules was determined using the antibody against acetylated α-tubulin; the position of the cleavage furrow always correlated with a rootlet microtubule in dividing *bld2-1* cells ($n = 40$). Light microscopic examination of *bld2–1* cells showed that the cleavage furrow was placed such that unequally sized sister cells were often produced. The area of cells in wild-type and *bld2-1* cultures was measured and the difference in area between sister cells and between unrelated (nonsister) cells was compared (Figure 6). In wild-type populations the mean difference in area between sisters (6.4 μm^2) was much less than between unrelated cells (15.3 μm^2). This suggests that the placement of the cleavage furrow in Chlamydomonas is nonrandom and generally results in two equal-sized cells. In *bld2-1* cells, the distribution of the mean differences in cell area between sister cells was similar to that of the mean difference between unrelated cells, which indicates that the areas of sister cells are not correlated to each other. Therefore, cleavage furrows are misplaced in *bld2-1* cells.

Spindle and cleavage furrow placement in *bld2-1* cells: We examined *bld2-1* cells to determine if the misplacement of the cleavage furrow was accompanied by a corresponding misplacement of the spindle, as observed in a *C. elegans par1* mutant strain (KEMPHUES *et al.* 1986). *bld2-1* cells exhibited a longer population doubling time in log phase cultures than wild-type cells (data not shown). A significant number of nondividing *bld2-1* cells with 0 or 2 nuclei was observed by DAPI staining when compared with *bld1-1* cells ($\chi^2 = 15.72$, $P < 0.001$; Table 2), which suggests that the spindle may no longer be oriented correctly in relation to the cleavage furrow. The pyrenoid, an easily visualized organelle located at the posterior end of the cell, was used as a cellular landmark. The orientation of the spindle was assessed by DAPI staining of the chromosomes, and the orientation of the cleavage furrow by phase microscopy. Only 25% of *bld2-1* cells examined had the normal orientation of the spindle and the cleavage furrow ($n = 81$, Figure 7). The spindle and cleavage furrow were misplaced with respect to each other in >36% of the scored cells. In relation to the pyrenoid, the spindle was oriented incorrectly in 48% of cells and the furrow was misplaced in 63% of cells. In the most extreme cases, the furrow was positioned parallel to the newly formed nuclei, such that the nuclei would have been cleaved or anucleate cells would have been formed (Figures 8 and 10, d and g).

Distribution of actin in relation to microtubule structures in mitotic cells: Actin microfilament networks are postulated to be involved in positioning the mitotic apparatus in other organisms. The dynamics of actin localization during mitosis in Chlamydomonas have been described previously; however, the distribution of actin
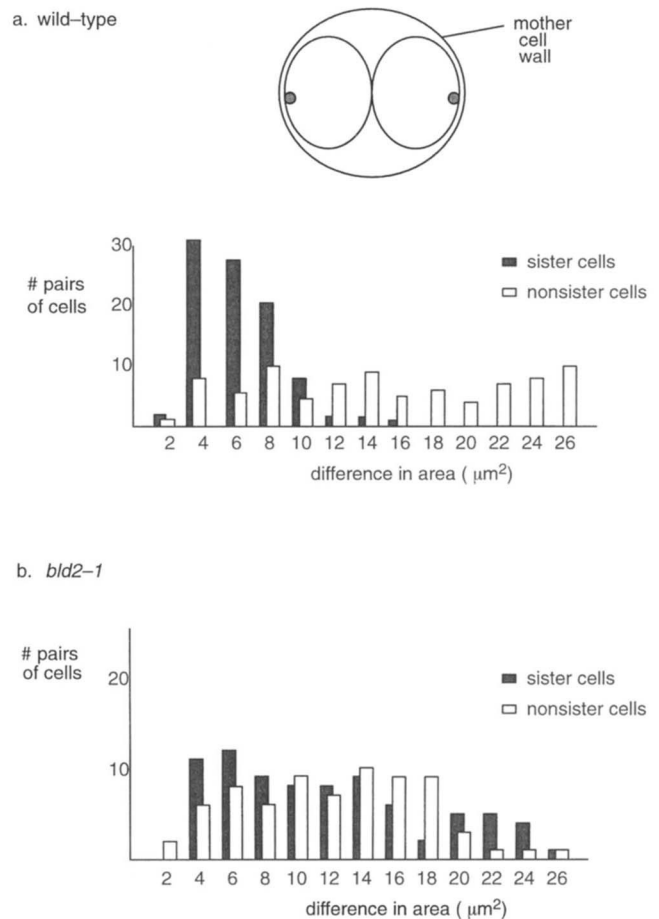

FIGURE 6.—Fidelity of cleavage furrow placement in wild-type and *bld2-1* cells. The difference in the area between sister cells, which are still within the mother cell wall, was compared with that between randomly selected single cells in the population. The random population represents cells at all stages of the cell cycle as opposed to the specific stage of the sister cells and therefore results in a relatively broad distribution of cell sizes. (a) Wild-type cells. The mean difference in area for sister cells was 6.4 μm^2 and the variance was 6.2 μm^2 ($n = 95$); for nonsister cell pairs the mean was 15.3 μm^2 and the variance was 57.8 μm^2 ($n = 87$). (b) *bld2-1* cells. The mean difference in area for sister cells was 11.93 μm^2 and the variance was 38.6 μm^2 ($n = 85$); for nonsister cell pairs the mean was 13.9 μm^2 and the variance was 52.5 μm^2 ($n = 85$). Area $= \pi wl$, where w = width of cell at widest point and l = length of cell at longest point.

in relationship to microtubule structures was not examined directly (HARPER *et al.* 1992). The distribution of actin in relation to the position of the spindle and rootlet microtubules during mitosis and cytokinesis in wild-type and in *bld2-1* cells was examined by immunofluorescence to determine if actin localization is correlated to the defect in positioning the spindle in *bld2-1* cells.

During preprophase in wild-type cells, the flagella were resorbed and cytoplasmic microtubules disassembled, the rootlet microtubules and basal bodies had not migrated, and the DNA was condensed. Actin colocalized with the proximal portions of the rootlet microtubules and in some cases was also in a ring around the

TABLE 2

The number of nuclei per cell in *bld1-1* and *bld2-1* strains

Strain	No. of nuclei per cell			Percent cells with abnormal no. of nuclei	χ^2
	0	1	2		
bld 1-1	0	384	11	2.8	
bld2-1	14	548	37	8.5	15.72

The number of nuclei per cell in both *bld 1-1* and *bld2-1* mutant strains was determined during log phase growth. Nuclei were visualized using DAPI to stain the DNA. Mitotic cells were not counted. The chi-square statistic used was a contingency test.

nucleus (Figure 9, a–c). In prophase, actin was distributed in a loosely defined ring or half ring around the forming spindle and colocalized with the rootlet microtubules that arced over the spindle (Figure 9, d–g). In prometaphase, actin was usually found in a full ring around the spindle and along the rootlet microtubules that continued to arc over the spindle (Figure 9, h–m). In metaphase, actin was distributed in a sharply defined ring around the spindle (Figure 9, n–q). In anaphase, a small cleavage furrow was sometimes apparent; actin colocalized with the rootlet microtubules and the incipient furrow (Figure 9, r–w). In cytokinesis, actin colocalized to the rootlet microtubules and the phycoplast, which were coincident with the cleavage furrow (data not shown).

The distribution of actin was altered during most stages of mitosis in *bld2-1* cells. During preprophase, actin localization was indistinguishable from that of wild-type cells (Figure 10, a–c). However, by prophase actin distribution became highly variable and did not appear as focused as in wild-type cells. Common localization patterns included half rings along one side of the spindle and along a rootlet

microtubule, along the rootlet microtubules only, or along rootlet microtubules and near the spindle but not in a ring (Figure 10, d–g). Ring patterns were often faint or diffuse; sharp rings such as those seen in wild-type cells were rarely observed. In prometaphase and metaphase, the actin distribution was also variable. It appeared both along rootlet microtubules and in diffuse rings or half rings along the spindle or appeared near but not along the spindle (Figure 10, h–k and l–q). The classic actin "metaphase ring" of wild-type cells was rarely observed and even then was less defined than in wild-type cells. However, cells with a wild-type appearing actin distribution did not necessarily have correct spindle placement (Figure 10, h–k). In anaphase, actin was concentrated along the rootlet microtubules but could also still be localized around part of the spindle (Figure 10, r–w). Although there appeared to be no overall consensus distribution of actin during most of mitosis in *bld2-1* cells, actin colocalized with the rootlet microtubules in all but one cell where rootlet microtubules were detected ($n = 27$).

The microtubule cytoskeleton of *bld2-1* cells was also disorganized during mitosis. The rootlet microtubules were mispositioned and could be present anywhere in the cell as opposed to the strict placement observed in wild-type cells. In particular, the rootlet microtubules rarely arced over the spindle as in wild-type cells (compare Figure 9d with Figure 10h). In some cells, the poles of the mitotic spindle were out of alignment with one another, so that the half spindles met off-center or at an angle in relation to each other. Rarely, monopolar or tripolar spindles were observed.

The distribution of centrin reorganizes during mitosis (SALISBURY *et al.* 1988). In wild-type cells, the centrin localization is near the basal bodies and the nuclear envelope. At metaphase, the majority of the staining is at the poles and centrin fibers emanate toward the spindle

	normal	DNA misplaced; furrow correct
wild–type:	84%	2%
bld2–1:	25%	12%

	DNA correct; furrow misplaced	DNA and furrow misplaced
wild–type:	2%	0%
bld2–1:	27%	36%
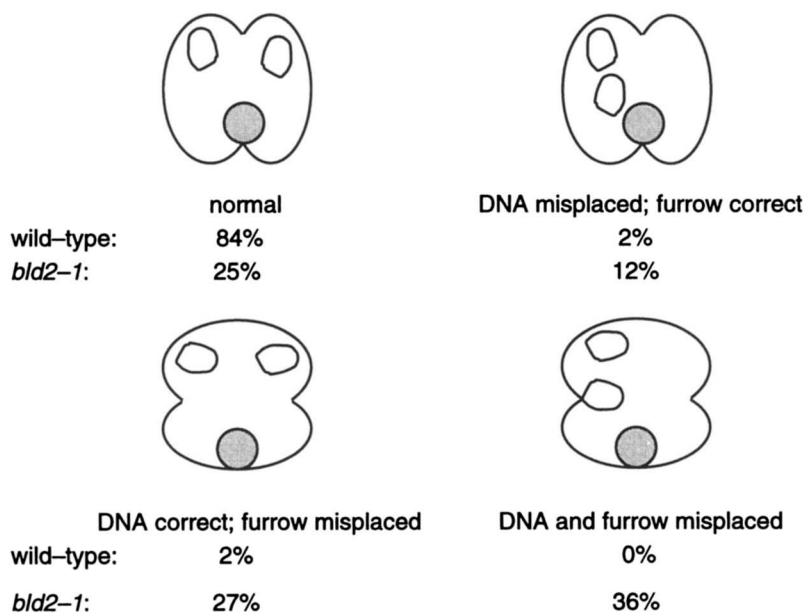
FIGURE 7.—Spindle and cleavage furrow misplacement in *bld2-1* cells. Diagrammatic representation of DNA position and cleavage furrow position in relation to the position of the pyrenoid in wild-type and *bld2-1* cells. The position of the DNA represents the orientation of the mitotic spindle; therefore two nuclei were required to make the assessment. Twelve percent of wild-type cells were unscorable; $n = 50$ for wild type, $n = 81$ for *bld2-1*.
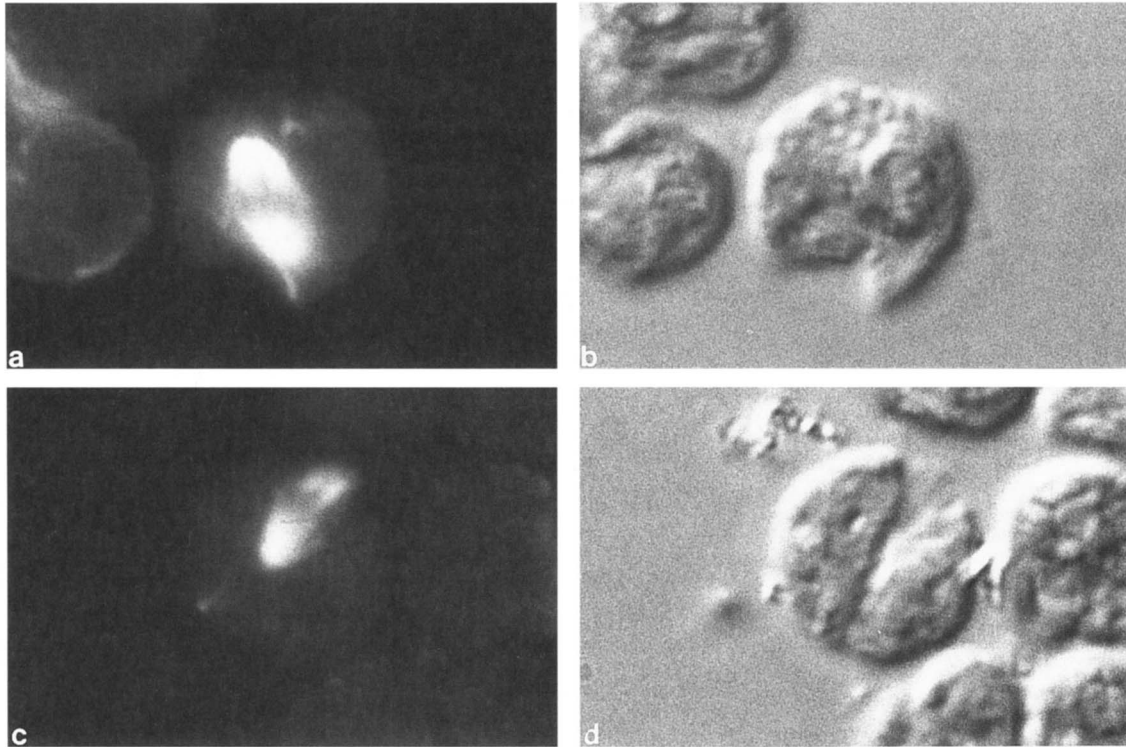
FIGURE 8.—Immunofluorescent images of spindle and cleavage furrow misplacement in *bld2-1* cells. (a and c) The cells were stained with anti-α-tubulin antibody and with FITC-conjugated secondary antibody. (b and d) Phase contrast images of cells. Note that the cleavage furrow was not perpendicular to the spindle in either cell. Bar, 10 μm.

microtubules (SALISBURY *et al.* 1988). We have examined the pattern of centrin staining during mitosis in *bld2-1* cells and found that the localization was similar to that in wild-type cells, although the staining that emanated toward the spindle may be reduced (data not shown).

Karyokinesis and cytokinesis are mistimed in *bld2-1* cells: In wild-type cells, the initiation of the cleavage furrow can occur as early as late anaphase (Figure 9u); more commonly the cleavage furrow initiates in telophase (GAFFEL and EL-GAMMEL 1990). *bld2-1* cells show a defect in coordinating karyokinesis and cytokinesis; cleavage furrows were observed at all nuclear stages of mitosis except preprophase (Figure 10, g and o; Table 3). Assuming cleavage furrows initiated in late anaphase are normal, 46% of *bld2-1* cells ($n = 46$) initiated cytokinesis at inappropriate stages of karyokinesis compared with wild-type cells (Table 3). When a furrow was present during an early stage of mitosis, actin was invariably concentrated along it and usually colocalized with a rootlet microtubule. Actin was often distributed along or near the spindle. Incorrect spindle placement did not depend on the presence of cleavage furrows during early mitotic stages. Some cells with furrows in an early mitotic stage had spindles positioned correctly, and some cells without furrows in an early mitotic stage had aberrantly positioned spindles.

DISCUSSION

Genetics of the *BLD2* locus: The *bld2-1* mutation represents a single allele at a previously unidentified locus

that maps to linkage group III. Based on this map position, the BLD2 gene product cannot be actin (C. SIL-FLOW, personal communication), α-tubulin (JAMES *et al.* 1993; A. M. PREBLE and S. K. DUTCHER, unpublished results), β-tubulin (BOLDUC *et al.* 1988), γ-tubulin (C. SILFLOW, personal communication), or centrin (TAILLON *et al.* 1992; K. MILLS and S. K. DUTCHER, unpublished results). Attempts to isolate additional alleles with similar phenotypes at the *BLD2* locus using standard mutageneses and screening for aflagellate cells have been unsuccessful. Among 250 independent aflagellate isolates, no alleles at the *BLD2* locus were recovered (S. K. DUTCHER, unpublished results). This may indicate that the *bld2-1* allele results in a rare phenotype for this locus. It is possible that the majority of mutations at the *BLD2* locus are lethal. Alternatively, it is possible that the *bld2-1* allele produces a recessive poison (antimorphic) gene product that results in a phenotype that other alleles do not display and that this phenotype is different from the null phenotype. Screens using the aflagellate phenotype as a basis for identifying new *bld2* alleles would fail in these cases. We believe it is unlikely that the *bld2-1* allele represents the null phenotype for this locus. The BLD2 gene product may be a structural component of the basal body or may be involved in the assembly of microtubule based structures. Although the BLD2 gene product could be a transcription factor for genes that encode basal body proteins, this seems unlikely in view of the new phenotypes in six of the intragenic revertants. Therefore, we
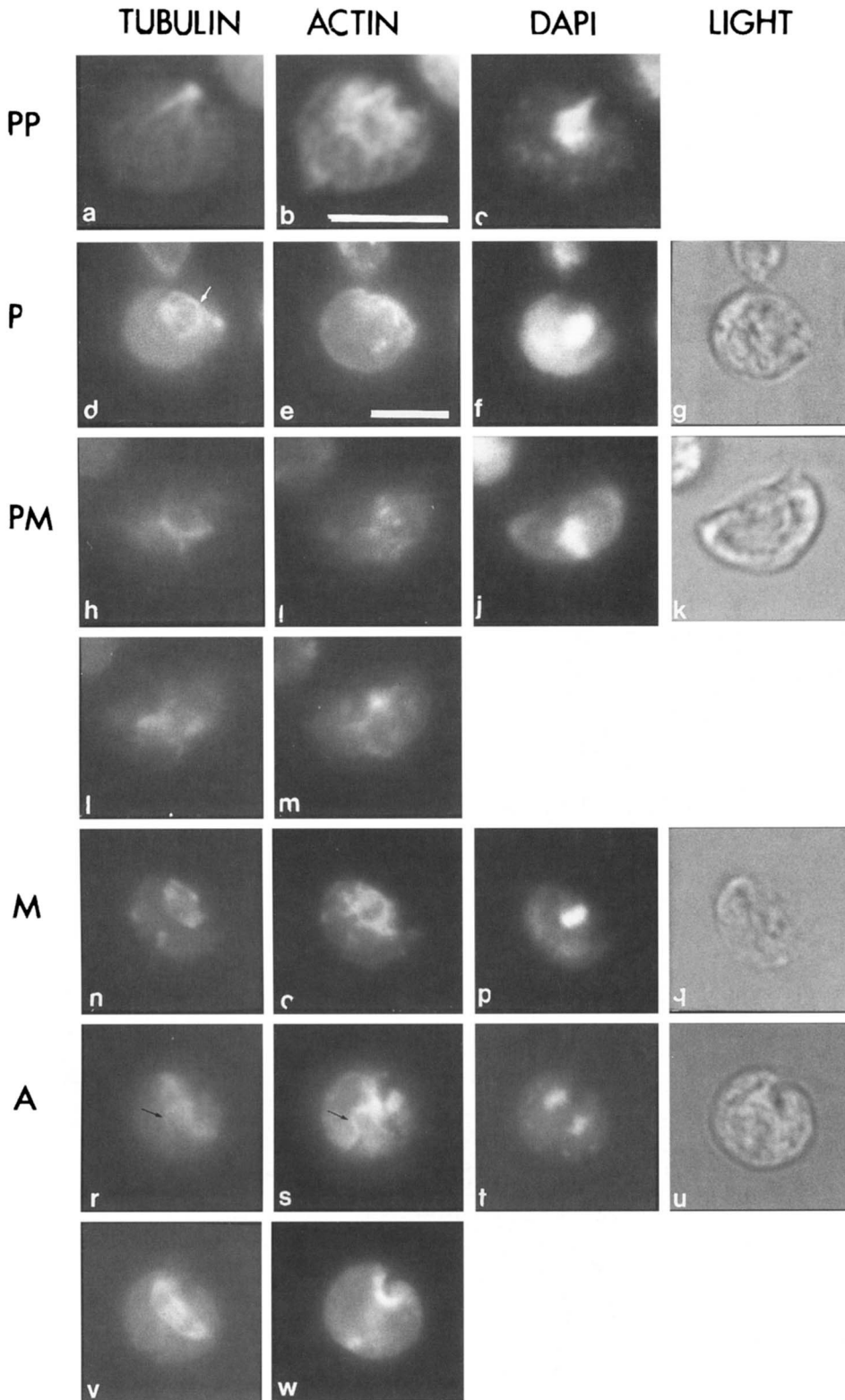
TUBULIN   ACTIN   DAPI   LIGHT

FIGURE 9.—The distribution of tubulin and actin during mitosis of wild-type cells. Cells were stained with anti-α-tubulin, anti-acetylated α-tubulin, and anti-actin primary antibodies and with Texas Red and FITC conjugated secondary antibodies (see MATERIALS AND METHODS). Due to the orientation of the cells, basal body staining cannot be seen in these images. Bars = 10 μm. (a–c) Pre-prophase. Actin was present in a ring around the nucleus and also colocalized to the proximal portions of the rootlet microtubules. (d–g) Prophase. Actin was present in a half ring around the spindle and was seen to follow a rootlet microtubule as it arced over the spindle (arrow). (h–m) Prometaphase (anterior view). (h) Anti-tubulin staining in the focal plane of the rootlet microtubules, (i) anti-actin staining in the same focal plane, (l) anti-tubulin staining in the focal plane of the spindle, and (m) anti-actin staining in the same focal plane. Actin staining colocalized with the rootlet microtubules, which curved over the spindle, and was also present in a ring around the spindle. The bright dots of actin seen in i that did not colocalize with the rootlet microtubules are part of the actin ring around the spindle. (n–q) Metaphase. Actin was in a prominent ring around the spindle; the distal portion of the rootlet microtubule seen in n was out of the focal plane. (r–w) Anaphase. (r) Anti-tubulin staining in the focal plane of a rootlet microtubule, (s) anti-actin staining in same focal plane, (v) anti-tubulin staining in the spindle focal plane, (w) anti-actin staining in the same focal plane. Actin staining followed the rootlet microtubule for its entire length (arrows); a cleavage furrow had initiated in this cell.

favor the hypothesis that the BLD2 gene product is a component of the basal bodies that is necessary for their assembly, although we cannot rule out other models or the possible separate requirement for the BLD2 gene product in flagellar assembly and cytokinesis.

The rootlet microtubules present during interphase in Chlamydomonas perform the functions of astral mi-crotubules during mitosis: In animal and some fungal cells, astral microtubules are present throughout mitosis and emanate from the mitotic poles toward the cell cortex, but are not part of the spindle itself. Astral microtubules (rays) are thought to have an important role in positioning the cleavage furrow during cell division (BEAMS and EVANS 1940; RAPPAPORT 1971, 1973; HAMA-
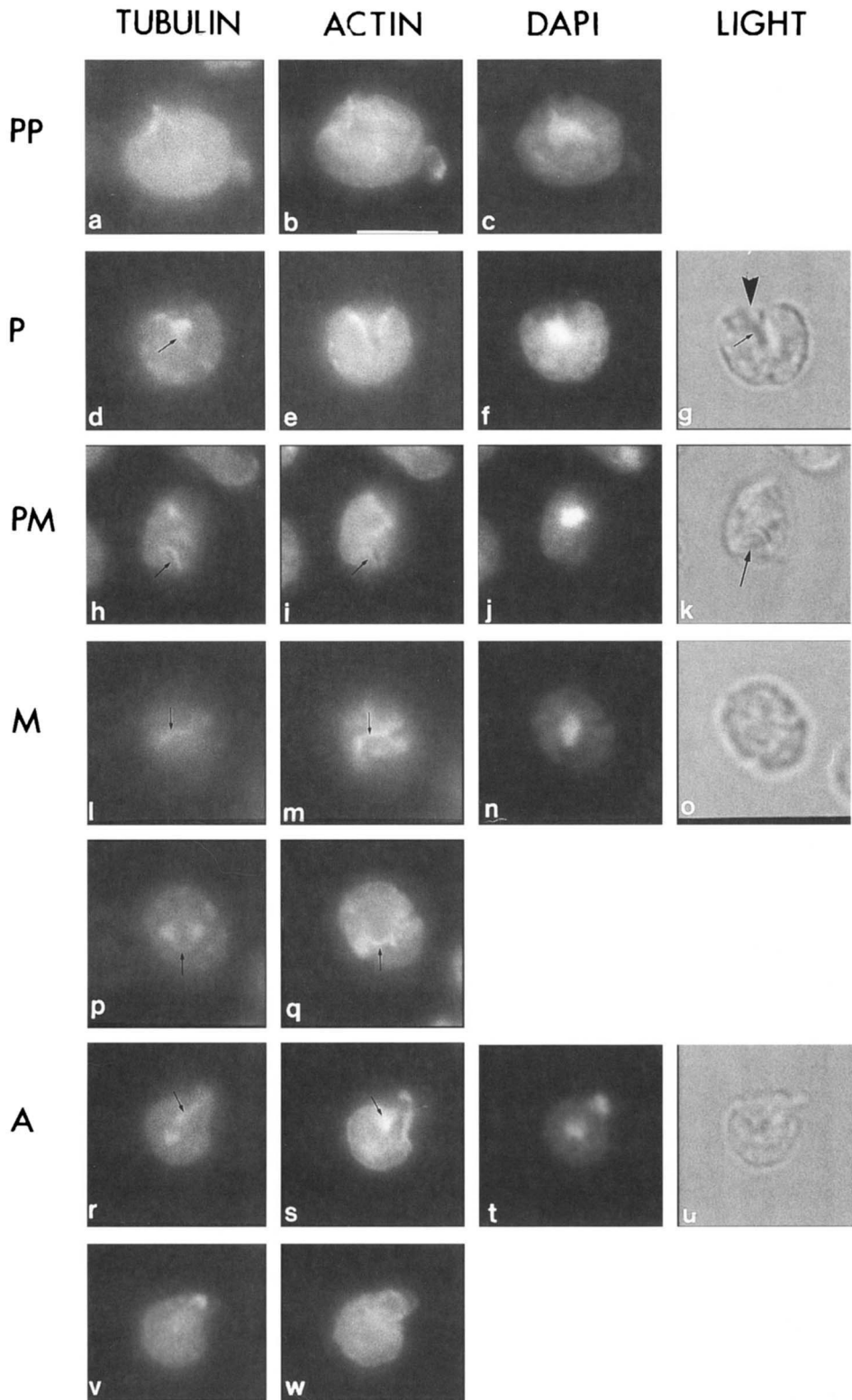
TUBULIN   ACTIN   DAPI   LIGHT

FIGURE 10.—The distribution of tubulin and actin during mitosis of *bld2-1* cells. Cells were stained with anti-α-tubulin, anti-acetylated α-tubulin, and anti-actin primary antibodies and with Texas Red and FITC conjugated secondary antibodies (see MATERIALS AND METHODS). Bar, 10 μm. (a–c) Preprophase. Actin localization was similar to that seen in wild-type at this stage. (d–g) Prophase. The second pole of the spindle seen in d was out of the plane of focus and was located at the anterior of the cell, just to the left of the rootlet microtubule. Actin was localized along the rootlet microtubule (arrows) that was associated with a prominent cleavage furrow (g, arrowhead) that did not bisect the spindle. This cytokinetic event would likely have resulted in the production of an anucleate cell. (h–k) Prometaphase. Actin was present in a half ring around the spindle and also colocalized to a rootlet microtubule (arrows in h and i). The spindle was not positioned perpendicular to the anterior-posterior axis of the cell as determined by the position of the pyrenoid (arrow in k). (l–q) Metaphase. (l) Anti-tubulin staining in the focal plane of a rootlet microtubule, (m) anti-actin in the same focal plane, (p) anti-tubulin staining in the focal plane of the spindle, (q) anti-actin in the same focal plane. Actin colocalized with both rootlet microtubules (arrows); a cleavage furrow has initiated in this cell. (r–v) Anaphase (anterior view). (r) Anti-tubulin staining in the focal plane of a rootlet microtubule positioned along the axis of the spindle. The spindle was positioned so that only one pole was in the plane of focus. (s) Anti-actin in the same focal plane, (v) anti-tubulin in the focal plane of the rest of the spindle, and (w) anti-actin in the same focal plane. Actin appeared to localize along the rootlet microtubule and along the side of the cell (arrows in r and s); it was also present in a ring around the top pole of the spindle.

GUCHI 1975; DEVORE *et al.* 1989; HARRIS and GEWALT 1989; reviewed in RAPPAPORT 1986; SATTERWAITE and POLLARD 1992; STROME 1993). The mitotic rootlet microtubules of Chlamydomonas are similar to astral microtubules and unlike the cytoplasmic microtubules that disassemble in preprophase. The rootlet microtubules are present throughout mitosis, originate in the centrosomes at the spindle poles, and are clearly not part of the spindle itself. In addition, the association between the rootlet microtubules and the position of the cleavage furrow is striking. In wild-type cells, actin colocalizes with the rootlets throughout mitosis and concentrates along them during anaphase and cytokinesis, and the position of the distal portions of the

TABLE 3

Mistiming of karyokinesis and cytokinesis in *bld2-1* cells

	No. of cells at mitotic stage[a]									
	Prophase		Prometaphase		Metaphase		Anaphase		Percent of total	
	bld2-1	wt	*bld2-1*	wt	*bld2-1*	wt	*bld2-1*	wt	*bld2-1*	wt
Furrow present	9	0	5	0	7	0	3	2	47	8
No furrow	13	9	4	2	8	10	2	3	53	92

Wild-type (wt; $n = 26$) and *bld2-1* cells ($n = 51$) were observed by indirect immunofluorescence using antibodies against both acetylated and nonacetylated α-tubulin and DNA was visualized by DAPI staining. The presence or absence of cleavage furrows was determined for cells that contained mitotic spindles.

[a] Cells in telophase normally may have initiated furrows, so this stage was not assessed independently from cytokinesis.

rootlet microtubules invariably predicts the position of the cleavage furrow. Although the overall distribution of actin in *bld2-1* cells during mitosis was variable, actin colocalized to the astral rootlet microtubules in 96% of cells, and cleavage furrows colocalized with rootlet microtubules even when the rootlet microtubules were aberrantly placed. The colocalization of actin with rootlet microtubules throughout mitosis indicated that the association of rootlet microtubules with cleavage furrows was not coincidental. This indicates that the rootlet microtubules play a role in positioning the cleavage furrow, and it is probable that the defect in cleavage furrow positioning seen in *bld2-1* cells is a result of the aberrant positioning of the astral rootlet microtubules and not of a defect in actin localization.

The centrosomal defect in *bld2-1* results in the mispositioning of the mitotic spindle via the astral microtubules: In *bld2-1* cells, the mitotic apparatus was positioned aberrantly in ≥48% of cells and mispositioning was observed in any stage of mitosis that had an assembled spindle. We suggest that this incorrect positioning resulted from centrosomes that are unable to maintain the normal cytoskeletal organization required for correct spindle orientation. In wild-type cells, the rootlet microtubules are maintained in a precise orientation relative to the basal bodies (RINGO 1967; WEISS 1984; GAFFEL and EL-GAMMEL 1990) and are normally linked to the basal bodies via the striated root fibers (WEISS 1984); this linkage is not possible in *bld2-1* cells. This cytoskeletal disorganization could directly result in the aberrant migration of the centrosomes, failure of the spindle to maintain a correct position, or both. It is clear from experiments in other organisms that astral microtubules have a significant role in both establishing and maintaining spindle position (HYMAN and WHITE 1987; HUFFAKER *et al.* 1988; HYMAN 1989; SULLIVAN and HUFFAKER 1992). The occasional displaced spindle halves, and monopolar and tripolar spindles observed during mitosis further indicated the deficiency of centrosomal organization in *bld2-1* cells, whereas the spindle itself appeared to function normally. The spindle positioning and anucleate/binucleate phenotypes exhibited by *bld2-1* cells are similar to the phenotypes

of a *Saccharomyces cerevisiae* β-tubulin mutation *tub2-401*. The loss of astral microtubules observed at the restrictive temperature in *tub2-401* strains is accompanied by mispositioning of the spindle and the production of anucleate and multinucleate cells; however, the actin microfilament network is apparently functional, as the cells continue the cell cycle (SULLIVAN and HUFFAKER 1992).

Many lines of evidence support the model that actin microfilaments have an important role in the positioning of the mitotic apparatus via the astral microtubules (HYMAN and WHITE 1987; PALMER *et al.* 1992; WADDLE *et al.* 1994). For example, at the restrictive temperature an *act1-4* mutant strain of *S. cerevisiae* shows complete loss of actin cables and randomization of the few cortical actin patches remaining (DUNN and SHORTLE 1990; PALMER *et al.* 1992). Actin disorganization is accompanied by the failure to maintain spindle position at the restrictive temperature (PALMER *et al.* 1992). Aside from the positioning defect, the microtubule cytoskeleton of *act1-4* cells appears normal during mitosis (PALMER *et al.* 1992). Therefore, alteration of either astral microtubules or actin microfilaments results in the mispositioning of the mitotic spindle, but the disruption of one of the cytoskeletal networks does not necessarily affect the integrity of the other.

In contrast, the disorganization of rootlet microtubules and the spindle positioning defect in *bld2-1* cells was accompanied by abnormal localization of actin. In wild-type cells, migration of the centrosomes occurs in preprophase and prophase (GAFFEL and EL-GAMMEL 1990); actin localizes mainly to the rootlets before centrosome migration. In *bld2-1* cells, there was wild-type localization of actin before centrosomal migration and abnormal actin localization was observed only after the centrosomes attempted to migrate. This abnormal actin localization was observed as a failure either to make or maintain the actin metaphase ring. However, *bld2-1* cells continued to localize actin to the rootlet microtubules during mitosis and showed no defect in the completion of cytokinesis, which indicates that the actin cytoskeleton was at least partially functional. Therefore, if actin is involved in the positioning of the spindle via the rootlet microtubules in Chlamydomonas

(as proposed by HARPER *et al.* 1992), it is likely that the lack of basal bodies disrupts the cytoskeletal architecture needed to maintain the orientation of the astral rootlet microtubules with the forming spindle, which results in the mispositioning of the spindle and the apparent abnormal actin distribution. We propose that the lack of basal bodies in the mitotic centrosome leads to the observed defects in actin localization and spindle and astral rootlet microtubule positioning.

Karyokinesis and cytokinesis are uncoupled in *bld2-1* cells: The presence of cleavage furrows during early stages of mitosis in *bld2-1* cells suggests a defect in the timing of cytokinesis with nuclear division. Uncoupling of karyokinesis and cytokinesis could result from the loss of a checkpoint control mechanism or the disruption/delay of a crucial event that occurs after the independence of the two pathways has been established. In previous studies of mitosis in wild-type Chlamydomonas, the addition of hydroxyurea blocks the completion of DNA replication and the subsequent formation of a spindle, but cleavage furrows are still initiated (HARPER and JOHN 1986). This suggests that cytokinesis proceeds independently of DNA replication and karyokinesis once a commitment to divide has been achieved. This experiment also suggests that there is not a checkpoint function that links DNA replication and spindle formation with cytokinesis. This result is unlike the situation in *S. cerevisiae,* where both cytokinesis and karyokinesis are blocked by a checkpoint until the DNA is correctly replicated (HARTWELL and WEINERT 1989). In addition, treatment of wild-type Chlamydomonas cells with vinblastine for 24-hr shifts the majority of the population to a 2C or greater ploidy of DNA. Treated cells are uninucleate and do not form spindles, but >30% of the cells initiate at least one cleavage furrow (A. R. SCHUTZ, L. L. EHLER, and S. K. DUTCHER, unpublished observations). This experiment suggests that there is not a microtubule-dependent cell-cycle block to cytokinesis and provides additional evidence that there is not a G$_2$ or M phase checkpoint that links karyokinesis with cytokinesis in Chlamydomonas. Therefore, it is likely that the uncoupling of karyokinesis and cytokinesis observed in *bld2-1* cells is due to a disruption/delay of an event that occurs after the pathways have separated.

One possible role of the centriole/basal body is to maintain cytoskeletal organization during cell division: The role of the centriole/basal body in cell division has been under investigation for many years. The isolation of cell lines lacking centrioles showed that centrioles are not essential for cell division and called into question the idea that they were necessary at all. Recently, *in vitro* studies have led to the hypothesis that centrioles provide a templating function necessary for the assembly of microtubules in cells. Experiments using the Xenopus sperm centrosome suggest that γ-tubulin is necessary but not sufficient for the nucleation of microtubules (FÉLIX *et al.* 1994; STEARNS and KIRSHNER 1994); a role of centrioles

in initiating or stabilizing the formation of microtubules was proposed. However, it is clear from this study that centrioles/basal bodies are not necessary for the nucleation of cytoplasmic, rootlet/astral, or spindle microtubules during the mitotic cell cycle in Chlamydomonas. Rather, it appears that the role of the centriole in some cell types may be to provide an organized cytoskeletal superstructure that is critical for the correct placement of the spindle and the cleavage furrow during cell division.

LITERATURE CITED

ARMBURST, E. V., P. J. FERRIS and U. W. GOODENOUGH, 1993 A mating type-linked gene cluster expressed in Chlamydomonas zygotes participates in the uniparental inheritance of the chloroplast genome. Cell 74: 801–811.

BEAMS, H. W., and T. C. EVANS, 1940 Some affects of colchicine upon the first cleavage in *Arbacia punctulata.* Biol. Bull. 79: 188–198.

BOLDUC, C., D. L. VINCENT and B. HUANG, 1988 β-tubulin mutants of the unicellular green alga *Chlamydomonas reinhardtii.* Proc. Natl. Acad. Sci. USA 85: 131–135.

CALARCO-GILLAM, P. D., M. C. SIEBERT, R. HUBBLE, T. MITCHISON and M. KIRSCHNER, 1983 Centrosome development in early mouse embryos as defined by an autoantibody against pericentriolar material. Cell 35: 621–629.

CHENG, N. N., C. M. KIRBY and K. J. KEMPHUES, 1995 Control of cleavage spindle orientation in *Caenorhabditis elegans:* the role of the genes *par-2* and *par-3.* Genetics 139: 549–559.

DEBEC, A., 1984 Evolution of karyotype in haploid cell lines of *Drosophila melanogaster.* Exp. Cell Res. 151: 236–246.

DEBEC, A., A. SZÖLLÖSI and D. SZÖLLÖSI, 1982 A Drosophila melanogaster cell line lacking centrioles. Cell 44: 133–138.

DEVORE J. J., G. W. CONRAD and R. RAPPAPORT, 1989 A model for astral stimulation of cytokinesis in animal cells. J. Cell Biol. 109: 2225–2232.

DUNN, T. M., and D. SHORTLE, 1990 Null alleles of SAC7 suppress temperature-sensitive actin mutations in *Saccharomyces cerevisiae.* Mol. Cell. Biol. 10: 2308–2314.

DUTCHER, S. K., 1995 Mating and tetrad analysis in *Chlamydomonas reinhardtii.* Methods Cell Biol. 47: 531–540.

DUTCHER, S. K., B. HUANG and D. J. L. LUCK, 1984 Genetic dissection of the central pair microtubules of the flagella of *Chlamydomonas reinhardtii.* J. Cell Biol. 98: 229–236.

ESHEL, D., L. A. URRESTARAZU, S. VISSERS, J. C. JAUNIAUX, J. C. VAN VLIET-REEDJIK *et al.,* 1993 Cytoplasmic dynein is required for normal nuclear segregation in yeast. Proc. Natl. Acad. Sci. USA 90: 11172–11176.

FÉLIX, M.-A., C. ANTONY, M. WRIGHT and B. MARO, 1994 Centrosome assembly in vitro: role of γ-tubulin recruitment in *Xenopus* sperm aster formation. J. Cell Biol. 124: 19–31.

FULTON, C., and A. D. DINGLE, 1971 Basal bodies but not centrioles, in *Naegleria.* J. Cell Biol. 51: 826–836.

GAFFEL, G. P., and S. EL-GAMMEL, 1990 Elucidation of the enigma of the "metaphase band" of *Chlamydomonas reinhardtii.* Protoplasma 156: 139–148.

GARDNER, L. C., E. O'TOOLE, C. A. PERRONE, T. GIDDINGS and M. E. PORTER, 1994 Components of a "dynein regulatory complex" are

located at the junction between the radial spokes and the dynein arms in *Chlamydomonas* flagella. J. Cell Biol. **127:** 1311–1326.

GILL, S. R., T. A. SCHOER, I. SZLAK, E. R. STEUER, M. P. SHEETZ *et al.*, 1991 Dynactin, a conserved, ubiquitously expressed component of an activator of vesicle motility mediated by cytoplasmic dynein. J. Cell Biol. **115:** 1639–1650.

GOODENOUGH, U. W., and H. S. ST. CLAIR, 1975 bald-2: a mutation affecting the formation of doublet and triplet sets of microtubules in *Chlamydomonas reinhardtii.* J. Cell Biol. **66:** 480–491.

GOODENOUGH, U. W., and R. L. WEISS, 1978 Interrelationships between microtubules, a striated fiber, and the gametic mating structure of *Chlamydomonas reinhardtii.* J. Cell Biol. **76:** 480–483.

GOULD, R. R., 1975 The basal bodies of *Chlamydomonas reinhardtii:* formation from probasal bodies, isolation, and partial characterization. J. Cell Biol. **65:** 65–74.

GOULD, R. R., and G. G. BORISY, 1977 The pericentriolar material in Chinese hamster ovary cells nucleates microtubule formation. J. Cell Biol. **73:** 601–615.

GROSS, C. H., L. P. W. RANUM and P. A. LEFEBVRE, 1988 Extensive restriction fragment length polymorphisms in a new isolate of *Chlamydomonas reinhardtii.* Curr. Genet. **13:** 503–508.

HAMAGUCHI, Y., 1975 Microinjection of colchicine into sea urchin eggs. Dev. Growth Differ. **17:** 111–117.

HARPER, J. D. I., and P. C. L. JOHN, 1986 Coordination of division events in the *Chlamydomonas* cell cycle. Protoplasma **131:** 118–130.

HARPER, J. D. I., D. W. McCURDY, M. A. SANDERS, J. L. SALISBURY, and P. C. JOHN, 1992 Actin dynamics during the cell cycle in *Chlamydomonas reinhardtii.* Cell Motil. Cytoskeleton **22:** 117–126.

HARRIS A. K., and S. L. GEWALT, 1989 Simulation testing of mechanisms for inducing the formation of the contractile ring in cytokinesis. J. Cell Biol. **109:** 2215–2224.

HARRIS, E. H., 1989 *The Chlamydomonas Sourcebook, a Comprehensive Guide to Biology and Laboratory Use.* Academic Press, San Diego, CA.

HARTWELL, L. H., and T. A. WEINERT, 1989 Checkpoints: controls that ensure the order of cell cycle events. Science **246:** 629–633.

HILL, D. P., and S. STROME, 1988 An analysis of the role of microfilaments in the establishment and maintenance of asymmetry in *Caenorhabditis elegans* zygotes. Dev. Biol. **124:** 75–84.

HILL, D. P., and S. STROME, 1990 Brief cytochalasin-induced disruption of microfilaments during a critical interval in 1-cell *C. elegans* embryos alters the partitioning of developmental instructions to the 2-cell embryo. Development **108:** 159–172.

HOLMES, J. A., and S. K. DUTCHER, 1989 Cellular asymmetry in *Chlamydomonas reinhardtii.* J. Cell Sci. **94:** 273–285.

HUFFAKER, T. C., J. H. THOMAS and D. BOTSTEIN, 1988 Diverse effects of beta-tubulin mutations on microtubule formation and function. J. Cell Biol. **106:** 1997–2010.

HYMAN, A. A., 1989 Centrosome movement in the early divisions of *Caenorhabditis elegans:* a cortical site determining centrosome position. J. Cell Biol. **109:** 1185–1193.

HYMAN, A. A., and J. G. WHITE, 1987 Determination of cell division axes in the early embryogenesis of *Caenorhabditis elegans.* J. Cell Biol. **105:** 2123–2135.

JAMES, S. W., C. D. SILFLOW, P. STROOM and P. A. LEFEBVRE, 1993 A mutation in the α1-tubulin gene of *Chlamydomonas reinhardtii* confers resistance to anti-microtubule herbicides. J. Cell Sci. **106:** 209–218.

JOHNSON, U. G., and K. R. PORTER, 1968 Fine structure of cell division in *Chlamydomonas reinhardtii.* J. Cell Biol. **38:** 403–425.

KEMPHUES, K. J., N. WOLF, W. B. WOOD and D. HIRSH, 1986 Two loci required for cytoplasmic organization in early embryos of *Caenorhabditis elegans.* Dev. Biol. **113:** 449–460.

KEMPHUES, K. J., J. R. PRIESS, D. G. MORTON and N. S. CHENG, 1988 Identification of genes required for cytoplasmic localization in early C. elegans embryos. Cell **52:** 311–320.

LEDIZET, M., and G. PIPERNO, 1986 Cytoplasmic microtubules containing acetylated alpha-tubulin in *Chlamydomonas reinhardtii:* spatial arrangement and properties. J. Cell Biol. **103:** 13–22.

LI, Y. Y., E. YEH, T. HAYS and K. BLOOM, 1993 Disruption of mitotic spindle orientation in a yeast dynein mutant. Proc. Natl. Acad. Sci. USA **90:** 10096–11000.

LUCK, D., G. PIPERNO, Z. RAMANIS and B. HUANG, 1977 Flagellar mutants of *Chlamydomonas:* studies of radial spoke-defective strains by dikaryon and revertant analysis. Proc. Natl. Acad. Sci. USA **74:** 3456–3460.

LUX, F. G., III, and S. K. DUTCHER, 1991 Genetic interactions at the *FLA10* locus: suppressors and synthetic phenotypes that affect the cell cycle and flagellar function in *Chlamydomonas reinhardtii.* Genetics **128:** 549–561.

MANIOTIS, A., and M. SCHLIWA, 1991 Microsurgical removal of centrosomes blocks cell reproduction and centriole generation in BSC-1 cells. Cell **67:** 495–504.

McMILLAN, J. N., and K. TATCHELL, 1994 The *JNM1* gene in the yeast *Saccharomyces cerevisiae* is required for nuclear migration and spindle orientation during the mitotic cell cycle. J. Cell Biol. **125:** 143–158.

MOESTRUP, Ø., 1978 On the phylogenetic validity of the flagellar apparatus in green algae and other chlorophyll a and chlorophyll b containing plants. Biosystems **10:** 117–144.

MUHUA, L., T. S. KARPOVA and J. A. COOPER, 1994 A yeast actin-related protein homologous to that in vertebrate dynactin complex is important for spindle orientation and nuclear migration. Cell **78:** 669–679.

PALMER, R. E., D. S. SULLIVAN, T. HUFFAKER and D. KOSHLAND, 1992 Role of astral microtubules and actin in spindle orientation and migration in the budding yeast, *Saccharomyces cerevisiae.* J. Cell Biol. **119:** 583–593.

PASQUALE, S. M., and U. W. GOODENOUGH, 1987 Cyclic AMP functions as a primary sexual signal in gametes of *Chlamydomonas reinhardtii.* J. Cell Biol. **105:** 2279–2292.

RAPPAPORT, R., 1961 Experiments concerning the cleavage in sand dollar eggs. J. Exp. Zool. **148:** 81–89.

RAPPAPORT, R., 1971 Reversal of cleavage inhibition in enchinoderm eggs. J. Exp. Zool. **176:** 249–255.

RAPPAPORT, R., 1973 On the rate of movement of the cleavage stimulus in sand dollar eggs. J. Exp. Zool. **183:** 115–119.

RAPPAPORT, R., 1986 Establishment of the mechanism of cytokinesis in animal cells. Int. Rev. Cytol. **105:** 245–281.

RINGO, D. L., 1967 Flagellar motion and fine structure of the flagellar apparatus in *Chlamydomonas.* J. Cell Biol. **33:** 543–571.

SAGER, R., and S. GRANICK, 1954 Nutritional control of sexuality in *Chlamydomonas reinhardtii.* J. Gen. Physiol. **37:** 729–742.

SALISBURY, J. L., A. T. BARON and M. A. SANDERS, 1988 The centrin-based cytoskeleton of *Chlamydomonas reinhardtii:* distribution in interphase and mitotic cells. J. Cell Biol. **107:** 635–641.

SATTERWAITE, L. L., and T. D. POLLARD, 1992 Cytokinesis. Curr. Opin. Cell Biol. **4:** 43–52.

SCHIBLER, M. J, and B. HUANG, 1991 The *col^R4* and *col^R15* β-tubulin mutations in *Chlamydomonas reinhardtii* confer altered sensitivities to microtubule inhibitors and herbicides by enhancing microtubule stability. J. Cell Biol. **113:** 605–614.

STARLING, D., and J. RANDALL, 1971 The flagella of temporary dikaryons of *Chlamydomonas reinhardtii.* Genet. Res. **18:** 107–113.

STEARNS, T., and M. KIRSCHNER, 1994 In vitro reconstitution of centrosome assembly and function: the central role of γ-tubulin. Cell **76:** 623–637.

STROME, S., 1993 Determination of cleavage planes. Cell **72:** 3–6.

SULLIVAN, D., and T. HUFFAKER, 1992 Astral microtubules are not required for anaphase b in *Saccharomyces cerevisiae.* J. Cell Biol. **119:** 379–388.

SZÖLLÖSI, A., H. RIS, D. SZÖLLÖSI and A. DEBEC, 1986 A centriole-free *Drosophila* cell line: a high voltage EM study. Eur. J. Cell Biol. **40:** 100–104.

TAILON, B. E., S. A. ALDER, J. P. SUHAN and J. W. JARVIK, 1992 Mutational analysis of centrin: an EF-hand protein associated with three distinct contractile fibers in the basal body apparatus of *Chlamydomonas.* J. Cell Biol. **119:** 1613–1624.

WADDLE, J. A., J. A. COOPER and R. H. WATERSTON, 1994 Transient localized accumulation of actin in *Caenorhabditis elegans* blastomeres with oriented asymmetric divisions. Development **120:** 2317–2328.

WEISS, R. L., 1984 Ultrastructure of the flagellar roots in *Chlamydomonas* gametes. J. Cell Sci. **67:** 133–143.

WITMAN, G. B., K. CARLSON, J. BERLINER and J. L. ROSENBAUM, 1972 *Chlamydomonas* flagella. I. Isolation and electrophoretic analysis of microtubules, matrix, membranes, and mastigonemes. J. Cell Biol. **54:** 507–539.

WRIGHT, R. L., J. L. SALISBURY and J. W. JARVIK, 1985 A nucleus-basal body connector in *Chlamydomonas reinhardtii* that may function in basal body localization or segregation. J. Cell Biol. **101:** 1903–1912.

Communicating editor: E. W. JONES